Effects of degradation products of biomedical magnesium alloys on nitric oxide release from vascular endothelial cells

Shuo Wang, Shi-Jie Zhu, Xue-Qi Zhang, Jing-An Li*, Shao-Kang Guan*
School of Material Science and Engineering & Henan Key Laboratory of Advanced Magnesium Alloy & Key Laboratory of Materials Processing and Mold Technology (Ministry of Education), Zhengzhou University, Zhengzhou, Henan Province, China

*Correspondence to: Jing-An Li, PhD, lijingan@zzu.edu.cn; Shao-Kang Guan, PhD, skguan@zzu.edu.cn.
orcid: 0000-0002-8311-1739 (Jing-An Li)

Abstract

Nitric oxide (NO) released by vascular endothelial cells (VECs), as a functional factor and signal pathway molecule, plays an important role in regulating vasodilation, inhibiting thrombosis, proliferation and inflammation. Therefore, numerous researches have reported the relationship between the NO level in VECs and the cardiovascular biomaterials' structure/functions. In recent years, biomedical magnesium (Mg) alloys have been widely studied and rapidly developed in the cardiovascular stent field for their biodegradable absorption property. However, influence of the Mg alloys' degradation products on VEC NO release is still unclear. In this work, Mg-Zn-Y-Nd, an Mg alloy widely applied on the biodegradable stent research, was investigated on the influence of the degradation time, the concentration and reaction time of degradation products on VEC NO release. The data showed that the degradation product concentration and the reaction time of degradation products had positive correlation with NO release, and the degradation time had negative correlation with NO release. All these influencing factors were controlled by the Mg alloy degradation behaviors. It was anticipated that it might make sense for the cardiovascular Mg alloy design aiming at VEC NO release and therapy.

Key words: nitric oxide; vascular endothelial cells; degradation products; Mg-Zn-Y-Nd alloy; cardiovascular stent; pro-endothelialization; anti-hyperplasia; anti-inflammation

doi: 10.4103/2045-9912.266991
How to cite this article: Wang S, Zhu SJ, Zhang XQ, Li JA, Guan SK. Effects of degradation products of biomedical magnesium alloys on nitric oxide release from vascular endothelial cells. Med Gas Res. 2019;9(3):153-159.
Funding: This study was funded by The Fostering Talents of National Natural Science Foundation of China and Henan Province (No. U1804251, to SKG), National Natural Science Foundation of China (No. NSFC51671175, to SJZ), Key Scientific and Technological Research Projects in Henan Province (No. 182102310076, to JAL), and Top Doctor Program of Zhengzhou University (No. 32210475, to JAL).

Introduction

Cardiovascular diseases caused by atherosclerosis and thrombosis have been the top threaten for human health worldwide for decades.[1] Current major strategies for the treatment of cardiovascular disease focus on cardiovascular stent intervention.[2] However, inevitable vascular wall damage after stent implantation tends to complicate the pathological biological processes, which ultimately leading to the risk of vessel restenosis and thrombosis.[3] Therefore, surface re-endothelialization becomes an ideal and effective strategy to avoid the pathological risk and prolong the stent life. Vascular endothelial cells (ECs) are important components of blood vessels, which play a particularly important role in maintaining the homeostasis of the cardiovascular system.[4-7] Nitric oxide (NO), produced by ECs oxidizing L-arginine through NO synthase, is a unique endogenous signal molecule in vascular biology.[8,9] Continuous release of NO from ECs can inhibit the migration and excessive proliferation of smooth muscle cells (SMCs) under pathological conditions and promote the healing of atherosclerotic lesions.[10-12] NO can reduce thrombosis via inhibiting platelets and erythrocytes aggregation, meanwhile promote ECs growth.[13,14]

As a potential material for absorbable cardiovascular stent, magnesium (Mg) alloy has received extensive attention in recent years.[15,16] Compared with permanent implants such as stainless steel stents and titanium alloy stents, Mg alloy cardiovascular stents will be absorbed after the expected function is completed, which not only avoids painful re-operation, but also greatly reduces the risk of long-term complications.[17] Nevertheless, excessive degradation property and limited pro-endothelialization are the bottlenecks in the development of Mg alloy stents.[18] At present, surface modification as an effective method to delay Mg alloys' degradation and improve their biocompatibility has attracted wide attention.[19-21] In addition, as a biodegradable material, the degradation products of Mg alloy contain a lot of Mg ion, which should promote the migration and growth of ECs.[22] Maier et al.[23] also reported that the Mg ion contributed to the synthesis of NO, in part through the up-regulation of endothelial NO synthase. However, the pro-endothelial function of the Mg alloy is still not satisfied till now. It was speculated that the parameters of degradation products, such as the degradation time, degradation product concentration and the reaction time of degradation products, may be the main factors affecting ECs growth and function (NO release). While little been reported on the above speculation, especially the effects of degradation products of Mg alloys on NO release from ECs.

In this contribution, Mg-Zn-Y-Nd alloy, as a biomass Mg alloy vascular scaffold material, was selected to investigate the effects of degradation products on NO release from ECs

because of its excellent mechanical properties and biocompatibility.[24,25] Compositions of degradation products of Mg-Zn-Y-Nd in different time periods and their effects on EC morphology, activity and NO release in different time periods were systematically investigated. This study is anticipated to guide significance to the potential of biodegradable Mg alloys in promoting NO release.

Materials and Methods

Materials

The Mg-Zn-Y-Nd alloy is produced in our laboratory (Henan Key Laboratory of Advanced Magnesium Alloy, Zhengzhou, China). The extruded Mg-Zn-Y-Nd alloy with a diameter of 10 mm was cut into a thickness of 3 mm by wire cutting. The samples were ground to 1000 grits with silicon carbide sandpaper and cleaned with anhydrous ethanol. The samples were stored in anhydrous ethanol for use.

Extract preparation

The extracts of Mg-Zn-Y-Nd samples which contained the degradation products were prepared according to ISO 10993-12: 2004. After ultraviolet sterilization, the samples were immersed in RPMI 1640 (Solabio, Beijing, China) medium containing 10% fetal bovine serum at the ratio of 1.25 cm^2/mL in cell culture incubator for 1 day (labeled as 100% 1d Extracts) and 3 days (labeled as 100% 3d Extracts).

Characterization of the corroded Mg-Zn-Y-Nd and the degradation products

The surface morphology of the leached samples before and after removal of the degradation products was observed by scanning electron microscopy (FEI Quanta 200, Eindhoven, Holland), and the elemental composition of each surface was also detected using the scanning electron microscopy matching energy dispersion spectrometer.[26] To investigate the mechanical property of the degraded Mg-Zn-Y-Nd alloy, surface hardness was detected as reported.[27] According to American Society for Testing Materials G1-03, the degradation products of surface deposition were removed by chromic acid solution for Mg alloy samples. The inductively coupled plasma optical emission spectrometry (ICP-OES, Agilent 5110, Palo Alto, CA, USA) was used to measure the concentration of Mg^{2+}, Zn^{2+}, Y^{3+}, Nd^{3+} in the extract and culture medium.

Co-culturing ECs with the degradation products of Mg-Zn-Y-Nd

To investigate the influence of degradation time, degradation product concentration and reaction time on the NO release from ECs. 100% 1d Extracts and 100% 3d Extracts were diluted to 20% (labeled as 20% 1d Extracts and 20% 3d Extracts), 40% (labeled as 40% 1d Extracts and 40% 3d Extracts), 60% (labeled as 60% 1d Extracts and 60% 3d Extracts), and 80% (labeled as 80% 1d Extracts and 80% 3d Extracts) with the cell culture medium and applied for culturing ECs for 1 day (24 hours) and 3 days (72 hours). The pure cell culture medium was used as control.

NO release

ECs (Chengdu Hao Yi Biotechnology Co., Ltd., Chengdu, China) were seeded at a density of 4×10^3 per well in a 96-well plate, and after the cells were completely confluent, the cells were cultured with the medium and the 20–100% concentration of the extract diluted with the medium. After 24 and 72 hours of incubation, the NO detection kit (Beyotime, Beijing, China) was used. In brief, the supernatant of cell culture, Griess Reagent I and Griess Reagent II were added into 96-well plate one by one with 50 μL each well, and then the absorbance was measured at 540 nm with a microplate reader (ThermoMultiskan MK3, Waltham, MA, USA).[13] For the measurement of standard curve, the absorbance was measured by the same method after diluting the standard to different concentrations in the medium.

As Li et al.[28] reported that the ECs regulated by the hyaluronic acid micro-strips could release more NO. Thus, in this experiment, NO released from the ECs which were regulated by the hyaluronic acid micro-strips (micro-pattern group) were detected as the positive control.[26]

To investigate the effect of the NO released from ECs in each group on anti-inflammation and anti-hyperplasia, the culture medium containing the NO released from ECs was collected from each group and was used to culture the macrophages and SMCs.[29] The macrophages and SMCs were stained with acridine orange/ethidium bromide (AO/EB), and living/dead cells were counted to evaluate the suppression effect of the NO on macrophages and SMCs.[30]

Cell proliferation evaluation

Cell viability was measured by 3-(4,5-dimethylthiazol-2-yl)-2,5-diphenyltetrazolium bromide assay kit (Solabio). Specifically, ECs were inoculated into 96-well plates at a density of 2×10^3 cells per hole for a period of time until the cells fully adhered to the culture plate. After 24 hours and 72 hours, the cells were cultured with the required solution.[31] The absorbance was measured at 492 nm according to the test instructions.

AO/EB staining of ECs

ECs were inoculated into 24-well plates at a density of 1.5×10^3 cells and cultured in the same way as above. Finally, the cells stained by AO/EB double-staining kit (Solabio) were observed by laser confocal microscopy (Nikon C2 Plus, Tokyo, Japan).[32]

Statistical analysis

The data are presented as the mean ± standard deviation (SD). Statistical analysis was applied as one-way analysis of variance followed by Tukey test, while *P*-values less than 0.05 suggesting significant difference. The OriginPro 2018 software (OriginLab, Northampton, MA, USA) was used in the study.

Results

Characterization of Mg-Zn-Y-Nd degradation products

Figure 1A showed the surface morphology of the Mg-Zn-Y-Nd alloy after immersed in the cell culture medium for 1 day and 3 days, respectively. At the 1st day, it could be seen numerous micro-particles on the Mg-Zn-Y-Nd, which may be composed of $CaCO_3$, $MgCO_3$, $Ca_3(PO_4)_2$ and $Mg_3(PO_3)_2$ (**Figure 1B**), while at the 3rd day, these micro-particles disappeared on

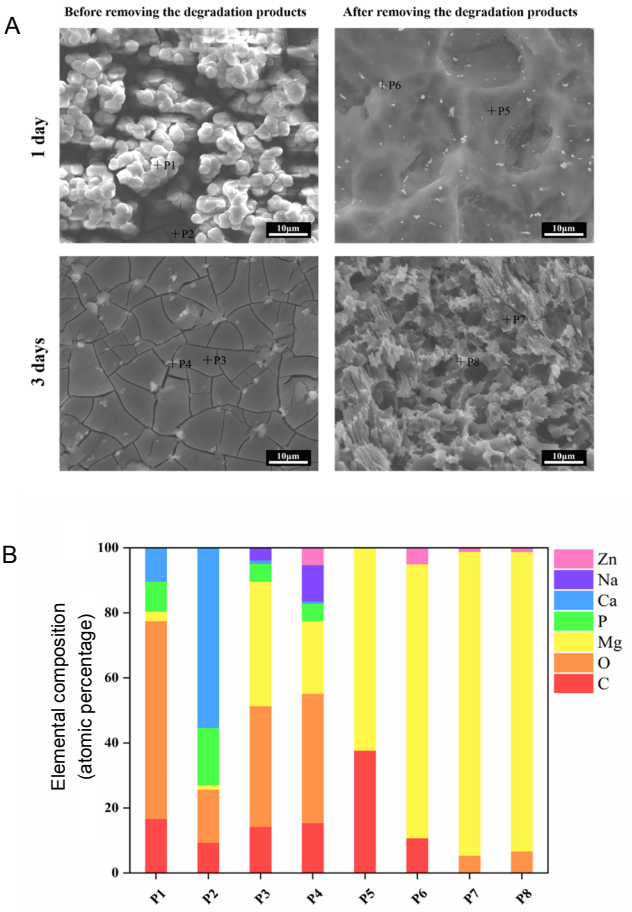

Figure 1: Morphology and elemental composition of the immersed Mg-Zn-Y-Nd.

Note: (A) Scanning electron microscope images of Mg-Zn-Y-Nd surface after immersed in the cell culture medium for 1 and 3 days. Scale bars: 10 μm. (B) The energy dispersive spectrometer of the typical area on the Mg-Zn-Y-Nd surface after immersed in the cell culture medium for 1 or 3 days.

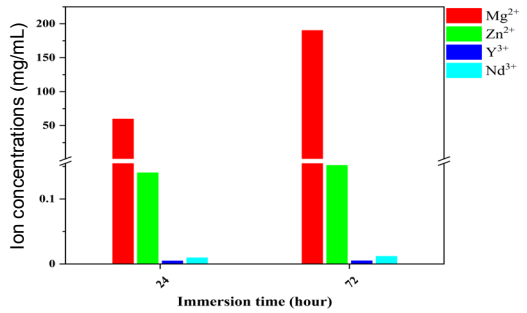

Figure 2: Inductively coupled plasma characterization of Mg^{2+}, Zn^{2+}, Y^{3+} and Nd^{3+} in the degradation products.

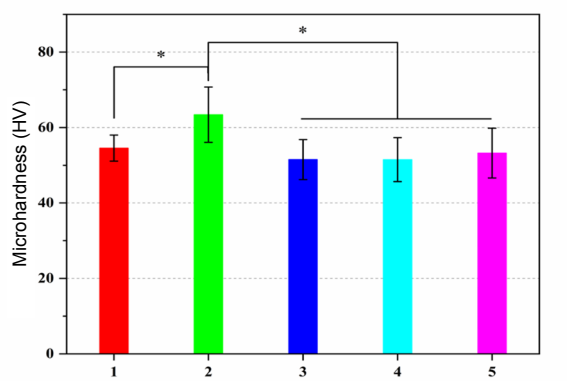

Figure 3: Micro-hardness of the un-degraded Mg-Zn-Y-Nd, and the Mg-Zn-Y-Nd alloy immersed in the culture medium for 1 and 3 days.

Note: Data are expressed as the mean ± SD (n = 10). *P < 0.05 (one-way analysis of variance). Sample 1: Un-degraded Mg-Zn-Y-Nd. Samples 2 and 3: Mg-Zn-Y-Nd immersed in the culture medium for 1 day. Samples 4 and 5: Mg-Zn-Y-Nd immersed in the culture medium for 3 days. Samples 2 and 4 were obtained before removing the degradation products; and samples 3 and 5 were obtained after removing the degradation products.

the surface. It was very likely to be peeled off and enter the extracts because the energy dispersive spectrometer showed that the Ca and Mg element also significantly reduced after 3 days' degradation. These micro-scaled particles were quite possible to influence the ECs growth and function, but they could not enter into the ECs to accelerate Mg delivery because their scales were bigger than 150 nm which was a threshold to permit the particles across. **Figure 2** showes that the main component of degradation products from Mg-Zn-Y-Nd was Mg^{2+} ions, possessing the concentration of 59.6 mg/mL at the 1st day and 190.1 mg/mL at the 3rd day. There were only small amounts of Zn^{2+} (0.14 mg/mL at the 1st day and 0.15 mg/mL at the 3rd day), Y^{3+} (0.0046 mg/mL at the 1st day and 0.0048 mg/mL at the 3rd day) and Nd^{3+} (0.009 mg/ml at the 1st day and 0.012 mg/mL at the 3rd day). Mg^{2+} contributes to ECs growth and functions, but the influence of the degradation time, degradation product concentration (Mg^{2+}) and the reaction time of degradation products on the growth and function (NO release) of ECs should be further investigated.

To study the influence of Mg-Zn-Y-Nd degradation on its mechanical property, the micro-hardness of the un-degraded Mg-Zn-Y-Nd, and the Mg-Zn-Y-Nd alloy immersed in the culture medium for 1 and 3 days were examined and displayed in **Figure 3**. The hardness significantly enhanced after being immersed in the culture medium for 1 day, which may be due to the absorption of Ca ion and the formation of the micro-scaled particles, because the hardness reduced to the same level as that of un-degraded Mg-Zn-Y-Nd after removing the micro-scaled particles. After immersing in the medium culture for 3 days, the micro-scaled particles fell off from the Mg-Zn-Y-Nd surface, and the exposed substrate maintained a consistent hardness with the un-degraded Mg-Zn-Y-Nd. Our data demonstrated that the absorbed Ca ion might enhance the surface hardness of the Mg-Zn-Y-Nd, which suggesting improved mechanical properties of degradation behavior.

Effects of degradation products on ECs growth and NO release

Figure 4 depicts the AO/EB images of the ECs. At the 1st day, the 1d Extracts groups made no markedly effects on the ECs growth, only 100% 1d Extracts group showed a lower ECs number compared to the control; at the 3rd day, 20% 1d Extracts, 40% 1d Extracts, 60% 1d Extracts and 80% 1d Extracts presented higher ECs numbers compared with the control, while the 100% 1d Extracts still showed the lower ECs number than the control group, which indicated the degradation product concentration could influence the ECs growth. However, the degradation time seemed to play more impor-

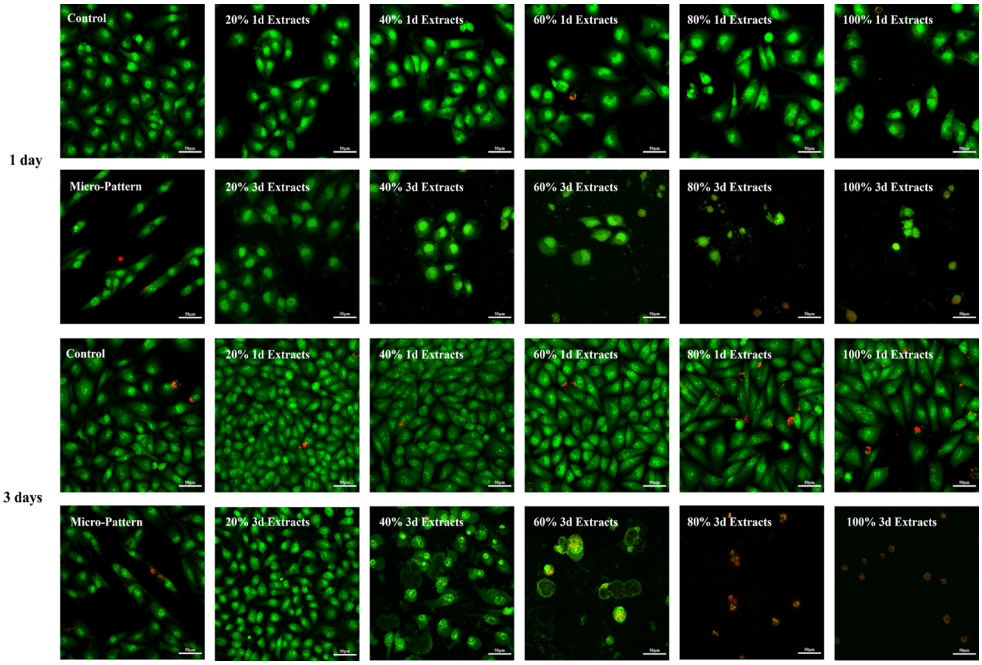

Figure 4: Acridine orange/ethidium bromide staining of endothelial cells co-cultured with different doses of Extracts for 1 and 3 days respectively.
Note: The green fluorescence marked cells indicated the healthy endothelial cells, and the red fluorescence marked cells represented apoptotic endothelial cells. Scale bars: 50 μm. 100% 1d/3d Extracts: The extracts of Mg-Zn-Y-Nd samples were immersed in RPMI 1640 medium containing 10% fetal bovine serum at the ratio of 1.25 cm^2/mL in cell culture incubator for 1 or 3 days.

tant role than the degradation product concentration on ECs growth. All the 3d Extracts groups showed lower ECs numbers compared to corresponding 1d Extracts, and the negative correlation between degradation product concentration and ECs growth was more evident in 3d Extracts groups: in the 80% 3d Extracts and 100% 3d Extracts groups, there were only a little red fluorescence marked cells.

The ECs in the micro-pattern group (positive control) presented elongated and spindle morphologies, and they grew along the micro-pattern's direction. Both on the 1st day and the 3rd day, the Micro-Pattern group presented higher ECs numbers compared with 100% 3d Extracts, 80% 3d Extracts, 60% 3d Extracts and 40% 3d Extracts groups, while lower ECs numbers compared to the other groups. The regulation of micro-pattern on ECs is an external factor,[14] which needs longer signal pathway. Most degradation products of Mg alloy own small scales which are less than 150 nm, and those small particles can pass the ECs membrane directly and regulate ECs internally.

Cell viability results displayed a trend of 100% 3d Extracts < 80% 3d Extracts < 60% 3d Extracts < 100% 1d Extracts < 40% 3d Extracts < control, 20% 1d Extracts, 40% 1d Extracts, 60% 1d Extracts and 80% 1d Extracts < 20% 3d Extracts at the 1st day, and 100% 3d Extracts and 80% 3d Extracts < 60% 3d Extracts < 100% 1d Extracts < 40% 3d Extracts < control and 80% 1d Extracts < 60% 1d Extracts and 20% 3d Extracts < 20% 1d Extracts and 40% 1d Extracts at the 3rd day. The degradation product concentration also showed negative correlation to ECs growth in 3d Extracts groups (**Figure 5**). Obviously, all the degradation time, degradation product concentration and the reaction time of degradation products made effects on the NO release from ECs.

Under the action of degradation products of Mg-Zn-Y-Nd, the NO release from ECs exhibited a completely different rule from cell viability (**Figure 6**): all the ECs in the degradation products groups released significantly more NO compared with the ECs in the control group and Micro-Pattern group, which indicated degradation products of Mg-Zn-Y-Nd promoted NO release from the ECs indeed; wherein, the degradation product concentration (20% Extracts, 40% Extracts, 60% Extracts, 80% Extracts, and 100% Extracts) and the reaction time of degradation products (co-culture with ECs for 1 day and 3 days) were positively correlated with the amount of the released NO (NO release trend: 20% Extracts < 40% Extracts < 60% Extracts < 80% Extracts < 100% Extracts; co-cultured for 1 day ≤ co-cultured for 3 days), and the degradation time (1d Extracts and 3d Extracts) was negatively correlated with NO release (NO release trend: 1d Extracts > 3d Extracts).

At the initial stage of degradation of Mg-Zn-Y-Nd, the main products are salts containing Mg ion. Therefore, Mg ion plays a crucial role on promoting NO release from the ECs. Recovery of adenosine triphosphate function is beneficial to the operation of sodium pump, which not only contributes to NO release from ECs but also promotes series of factors secretion, including prostaglandin, thrombomodulin, fibronectin, *etc*.[33] The recovery of adenosine triphosphate function depends on Mg ion.[26] With the degradation time going on, more elements, such as Zn, Y and Nd were released to the extracts. Although their influence on NO release from ECs is still unknown, our data showed that the NO release decreased with the degradation time going on (**Figure 6**, 1d Extracts > 3d Extracts). Another reason may be the scales of the Mg-Zn-Y-Nd degradation products, which have been described from nanometers to millimeters: small degradation products (scales < 150 nm) can cross the ECs membrane directly into the cell interior, while large degradation products cannot traverse the ECs membrane and the Mg ion's effect may be prevented;[34,35] initially degraded products are generally smaller in scale and thus favorable for cell absorption, while the scales of products degraded in later stage increases gradually, and then it is not conducive to the transport of Mg ions.

The SMCs and macrophages culture results showed negative

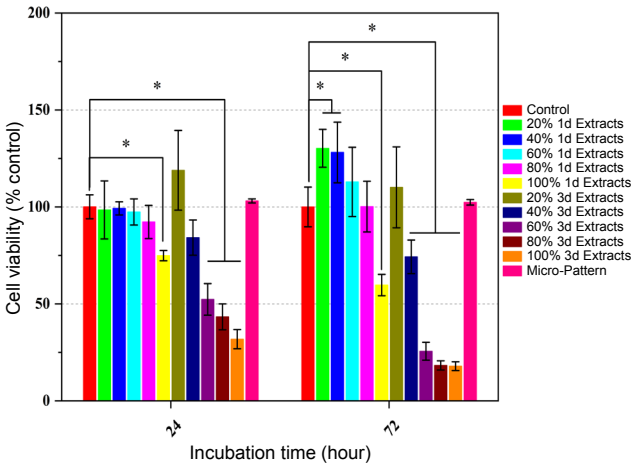

Figure 5: Viability of endothelial cells detected *via* a typical 3-(4,5-dimethylthiazol-2-yl)-2,5-diphenyltetrazolium bromide (MTT) assay.
Note: Data are expressed as the mean ± SD (n = 5). *P < 0.05 (one-way analysis of variance). 100% 1/3d Extracts: The extracts of Mg-Zn-Y-Nd samples were immersed in RPMI 1640 medium containing 10% fetal bovine serum at the ratio of 1.25 cm^2/mL in cell culture incubator for 1 or 3 days.

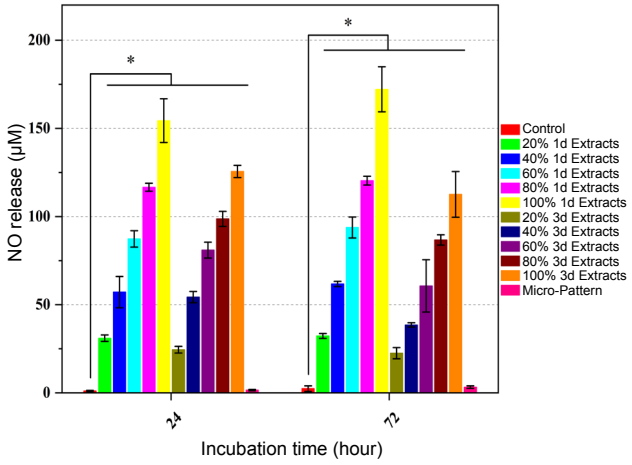

Figure 6: Nitric oxide release of endothelial cells detected *via* a typical Griess reagent assay.
Note: Data are expressed as the mean ± SD (n = 5). *P < 0.05 (one-way analysis of variance). 100% 1/3d Extracts: The extracts of Mg-Zn-Y-Nd samples were immersed in RPMI 1640 medium containing 10% fetal bovine serum at the ratio of 1.25 cm^2/mL in cell culture incubator for 1 or 3 days.

correlation trends compared to the NO released from the ECs in each group, which indicated that more NO release contributed to lower SMCs and macrophages viability. These results not only verified the NO function on anti-hyperplasia and anti-inflammation, but also revealed the Mg alloy degradation products inhibited inflammation and hyperplasia through the pathway of scale-endothelial regulation-NO release-SMCs/macrophage regulation (**Figures 7** and **8**).

Discussion

Mg alloys, as advanced materials, are highly expected in the field of biomedical materials due to their excellent mechanical properties and biodegradable absorption properties. However, it has rarely been reported on the interaction between degradation products of Mg alloys and human cells, especially about their regulation on the growth and NO release of vascular ECs in the field of cardiovascular biomaterials. Depending on lots of previous studies,[36-38] it was speculated that the regulation of the degradation products on ECs growth and NO release might be decided by the Mg alloys' degradation time, degradation product concentration and the reaction time of degradation products on ECs. Wherein, the degradation time determined the scales and components of the degradation products, as well as the micro-hardness of the Mg alloys. Our data also show that the scales, components and concentration of the degradation products may influence the ECs growth and NO release. The reaction time of the degradation products on the ECs also makes effects to their activity and NO release.

Li et al.[39] reported that the surface micro-pattern can simulate the effect of blood flow shear stress on ECs to elongate their morphologies and enhance their NO release. In this paper, the experimental results showed that the ECs in the 20% 1d Extracts and 40% 1d Extracts groups presented higher activ-

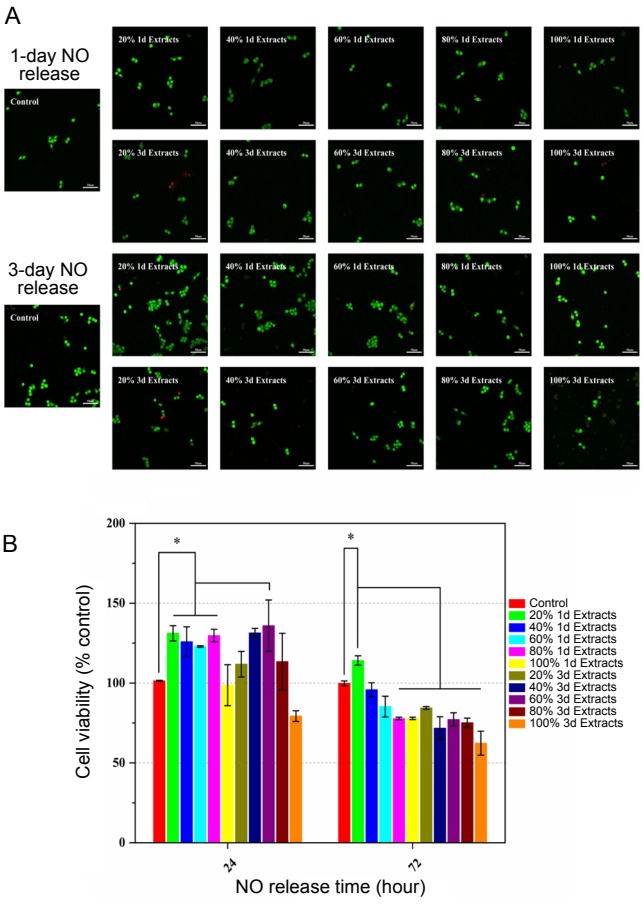

Figure 7: Nitric oxide (NO) impact on smooth muscle cells growth.
Note: (A, B) Acridine orange/ethidium bromide staining images (A) and vital ratios(B) of smooth muscle cells cultured with medium containing NO released by endothelial cells. Data are expressed as the mean ± SD (n = 5). *P < 0.05 (one-way analysis of variance). 100% 1d/3d Extracts: The extracts of Mg-Zn-Y-Nd samples were immersed in RPMI 1640 medium containing 10% fetal bovine serum at the ratio of 1.25 cm^2/mL in cell culture incubator for 1 or 3 days.

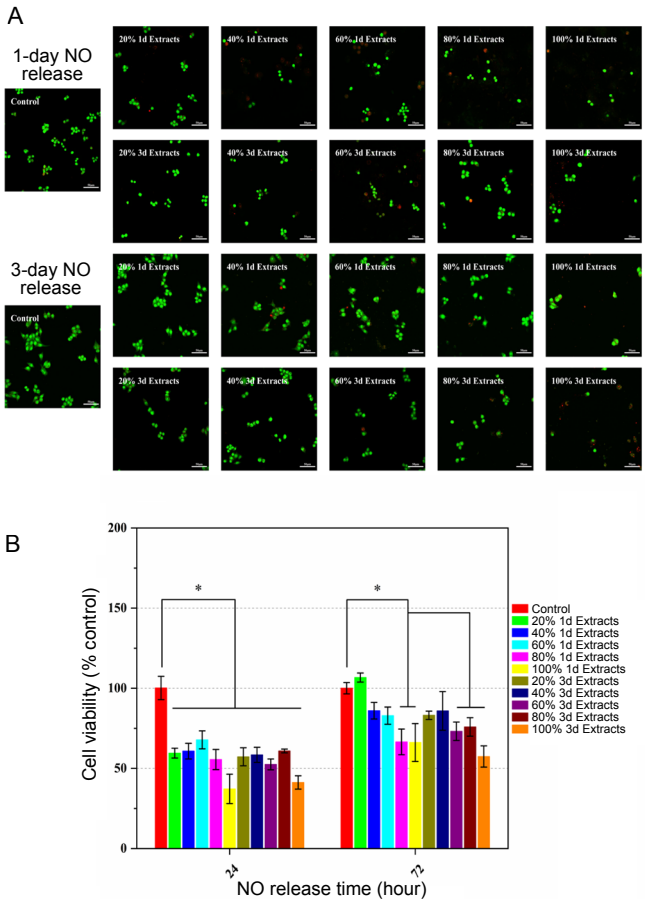

Figure 8: Nitric oxide (NO) impact on macrophages adhesion and growth. Note: (A, B) Acridine orange/ethidium bromide staining images (A) and vital ratios (B) of macrophages cultured with medium containing NO released by endothelial cells. Data are expressed as the mean ± SD (n = 5). *P < 0.05 (one-way analysis of variance). 100% 1d/3d Extracts: The extracts of Mg-Zn-Y-Nd samples were immersed in RPMI 1640 medium containing 10% fetal bovine serum at the ratio of 1.25 cm²/mL in cell culture incubator for 1 or 3 days.

ity than the ECs in the micro-pattern group, suggesting better ability on improving endothelial coverage. It is notable that the ECs in all the degradation products groups released more NO compared with the ECs in the micro-pattern group, ranging from several times to tens of times (**Figure 6**). These results suggested that the Mg alloys and their degradation products significantly made more effects on the NO release compared to surface topology.

NO, as an important gas, is a functional factor that released from vascular ECs, contributing to inhibiting hyperplasia and thrombosis. In the present study, we aimed to reveal the effects of degradation products of biodegradable stent material, Mg-Zn-Y-Nd, on NO release from ECs. The data suggested that the degradation product concentration and the reaction time of degradation products had positive correlation with NO release, and the degradation time had negative correlation with NO release. In addition, the degradation products also affected ECs growth, proliferation and apoptosis. These rules were attributed to the concentration of Mg ions, the composition and sizes of degradation products, respectively. These factors are ultimately influenced by degradation rate and mode of Mg-Zn-Y-Nd. We hope our research may provide design inspiration for Mg alloy stents and/or their modified coatings in the considerations of ECs NO release and therapy.

Author contributions
Literature search: SW, SJZ, JAL, SKG; manuscript preparation: SW, SJZ; experimental studies, and data acquisition: SW, XQZ; data analysis, statistical analysis, and manuscript editing: SW, JAL; intellectual content definition SJZ, JAL, SKG; manuscript review and guarantor: JAL, SKG. All authors approved the final manuscript for publication.
Conflicts of interest
There is no conflict of interest
Financial support
This study was funded by The Fostering Talents of National Natural Science Foundation of China and Henan Province, China (No. U1804251, to SKG), National Natural Science Foundation of China (No. NSFC51671175, to SJZ), Key Scientific and Technological Research Projects in Henan Province, China (No. 182102310076, to JAL), and Top Doctor Program of Zhengzhou University, China (No. 32210475, to JAL).

Data sharing statement
Data sets analyzed during the current study are available from the corresponding author on reasonable request.
Plagiarism check
Checked twice by iThenticate.
Peer review
Externally peer reviewed.

References

1. Piepoli MF, Hoes AW, Agewall S, et al. 2016 European Guidelines on cardiovascular disease prevention in clinical practice: The Sixth Joint Task Force of the European Society of Cardiology and Other Societies on Cardiovascular Disease Prevention in Clinical Practice (constituted by representatives of 10 societies and by invited experts) Developed with the special contribution of the European Association for Cardiovascular Prevention & Rehabilitation (EACPR). *Eur Heart J.* 2016;37:2315-2381.
2. Garg S, Serruys PW. Coronary stents: current status. *J Am Coll Cardiol.* 2010;56:S1-42.
3. Thottappillil N, Nair PD. Scaffolds in vascular regeneration: current status. *Vasc Health Risk Manag.* 2015;11:79-91.
4. Ferrara N. Vascular endothelial growth factor: basic science and clinical progress. *Endocr Rev.* 2004;25:581-611.
5. Cooke DL, McCoy DB, Halbach VV, et al. Endovascular biopsy: in vivo cerebral aneurysm endothelial cell sampling and gene expression analysis. *Transl Stroke Res.* 2018;9:20-33.
6. Chen J, Cui C, Yang X, et al. MiR-126 affects brain-heart interaction after cerebral ischemic stroke. *Transl Stroke Res.* 2017;8:374-385.
7. Blecharz-Lang KG, Wagner J, Fries A, et al. Interleukin 6-mediated endothelial barrier disturbances can be attenuated by blockade of the IL6 receptor expressed in brain microvascular endothelial cells. *Transl Stroke Res.* 2018;9:631-642.
8. Moncada S, Higgs A. The L-arginine-nitric oxide pathway. *N Engl J Med.* 1993;329:2002-2012.
9. Cai W, Wu J, Xi C, Meyerhoff ME. Diazeniumdiolate-doped poly(lactic-co-glycolic acid)-based nitric oxide releasing films as antibiofilm coatings. *Biomaterials.* 2012;33:7933-7944.
10. Napoli C, de Nigris F, Williams-Ignarro S, Pignalosa O, Sica V, Ignarro LJ. Nitric oxide and atherosclerosis: an update. *Nitric Oxide.* 2006;15:265-279.

11. Major TC, Brisbois EJ, Jones AM, et al. The effect of a polyurethane coating incorporating both a thrombin inhibitor and nitric oxide on hemocompatibility in extracorporeal circulation. *Biomaterials*. 2014;35:7271-7285.
12. Palmer RM, Ferrige AG, Moncada S. Nitric oxide release accounts for the biological activity of endothelium-derived relaxing factor. *Nature*. 1987;327:524-526.
13. Yang Z, Yang Y, Zhang L, et al. Mussel-inspired catalytic selenocystamine-dopamine coatings for long-term generation of therapeutic gas on cardiovascular stents. *Biomaterials*. 2018;178:1-10.
14. Qiu H, Qi P, Liu J, et al. Biomimetic engineering endothelium-like coating on cardiovascular stent through heparin and nitric oxide-generating compound synergistic modification strategy. *Biomaterials*. 2019;207:10-22.
15. Wang HX, Guan SK, Wang X, Ren CX, Wang LG. In vitro degradation and mechanical integrity of Mg-Zn-Ca alloy coated with Ca-deficient hydroxyapatite by the pulse electrodeposition process. *Acta Biomater*. 2010;6:1743-1748.
16. Wang P, Xiong P, Liu J, Gao S, Xi T, Cheng Y. A silk-based coating containing GREDVY peptide and heparin on Mg-Zn-Y-Nd alloy: improved corrosion resistance, hemocompatibility and endothelialization. *J Mater Chem B*. 2018;6:966-978.
17. Zheng YF, Gu XN, Witte F. Biodegradable metals. *Mater Sci Eng R Rep*. 2014;77:1-34.
18. Chen L, Li J, Wang S, et al. Surface modification of the biodegradable cardiovascular stent material Mg-Zn-Y-Nd alloy via conjugating REDV peptide for better endothelialization. *J Mater Res*. 2018;33:4123-4133.
19. Chen L, Li J, Chang J, et al. Mg-Zn-Y-Nd coated with citric acid and dopamine by layer-by-layer self-assembly to improve surface biocompatibility. *Science China Technological Sciences*. 2018;61:1228-1237.
20. Ma X, Zhu S, Wang L, Ji C, Ren C, Guan S. Synthesis and properties of a bio-composite coating formed on magnesium alloy by one-step method of micro-arc oxidation. *J Alloys Compd*. 2014;590:247-253.
21. Liu Y, Zheng Y, Chen X-H, et al. Fundamental theory of biodegradable metals—definition, criteria, and design. *Adv Funct Mater*. 2019;29:1805402.
22. Song X, Chang L, Wang J, et al. Investigation on the in vitro cytocompatibility of Mg-Zn-Y-Nd-Zr alloys as degradable orthopaedic implant materials. *J Mater Sci Mater Med*. 2018;29:44.
23. Maier JA, Bernardini D, Rayssiguier Y, Mazur A. High concentrations of magnesium modulate vascular endothelial cell behaviour in vitro. *Biochim Biophys Acta*. 2004;1689:6-12.
24. Wang J, Zhou Y, Yang Z, Zhu S, Wang L, Guan S. Processing and properties of magnesium alloy micro-tubes for biodegradable vascular stents. *Mater Sci Eng C Mater Biol Appl*. 2018;90:504-513.
25. Wu Q, Zhu S, Wang L, et al. The microstructure and properties of cyclic extrusion compression treated Mg-Zn-Y-Nd alloy for vascular stent application. *J Mech Behav Biomed Mater*. 2012;8:1-7.
26. Zou D, Luo X, Han CZ, et al. Preparation of a biomimetic ECM surface on cardiovascular biomaterials via a novel layer-by-layer decellularization for better biocompatibility. *Mater Sci Eng C Mater Biol Appl*. 2019;96:509-521.
27. Bai Y, Zhang K, Xu R, et al. Surface modification of esophageal stent materials by a drug-eluting layer for better anti-restenosis function. *Coatings*. 2018;8:215.
28. Li J, Zhang K, Wu J, et al. Tailoring of the titanium surface by preparing cardiovascular endothelial extracellular matrix layer on the hyaluronic acid micro-pattern for improving biocompatibility. *Colloids Surf B Biointerfaces*. 2015;128:201-210.
29. Wu F, Li J, Zhang K, et al. Multifunctional coating based on hyaluronic acid and dopamine conjugate for potential application on surface modification of cardiovascular implanted devices. *ACS Appl Mater Interfaces*. 2016;8:109-121.
30. Li J, Zhang K, Chen H, et al. A novel coating of type IV collagen and hyaluronic acid on stent material-titanium for promoting smooth muscle cell contractile phenotype. *Mater Sci Eng C Mater Biol Appl*. 2014;38:235-243.
31. Li J, Wu F, Zhang K, et al. Controlling molecular weight of hyaluronic acid conjugated on amine-rich surface: toward better multifunctional biomaterials for cardiovascular implants. *ACS Appl Mater Interfaces*. 2017;9:30343-30358.
32. Han C, Luo X, Zou D, et al. Nature-inspired extracellular matrix coating produced by micro-patterned smooth muscle and endothelial cells endows cardiovascular materials with better biocompatibility. *Biomaterials science*. 2019;7:2686-2701.
33. Xiang L, Li J, He Z, Wu J, Yang P, Huang N. Design and construction of TiO2 nanotubes in microarray using two-step anodic oxidation for application of cardiovascular implanted devices. *Micro Nano Lett*. 2015;10:287-291.
34. Nakamura S, Koga S, Shibuya N, Seo K, Kidokoro SI. A new multi-binding model for isothermal titration calorimetry analysis of the interaction between adenosine 5'-triphosphate and magnesium ion. *Thermochim Acta*. 2013;563:82-89.
35. Wang S, Li J, Zhou Z, Zhou S, Hu Z. Micro-/nano-scales direct cell behavior on biomaterial surfaces. *Molecules*. 2018;24:E75.
36. Alvarez F, Lozano Puerto RM, Pérez-Maceda B, Grillo CA, Fernández Lorenzo de Mele M. Time-lapse evaluation of interactions between biodegradable mg particles and cells. *Microsc Microanal*. 2016;22:1-12.
37. Gu X, Zheng Y, Cheng Y, Zhong S, Xi T. In vitro corrosion and biocompatibility of binary magnesium alloys. *Biomaterials*. 2009;30:484-498.
38. Fang Z, Zhao Y, Wang H, et al. Influence of surface charge density on ligand-metal bonding: A DFT study of NH3 and HCOOH on Mg (0 0 0 1) surface. *Appl Surf Sci*. 2019;470:893-898.
39. Li J, Zhang K, Yang P, et al. Human vascular endothelial cell morphology and functional cytokine secretion influenced by different size of HA micro-pattern on titanium substrate. *Colloids Surf B Biointerfaces*. 2013;110:199-207.

Received: May 29, 2019
Reviewed: May 30, 2019
Accepted: July 29, 2019